J Mater Sci (2009) 44:6453–6462
DOI 10.1007/s10853-009-3610-9

MESOSTRUCTURED MATERIALS

Morphological control on SBA-15 mesoporous silicas via a slow self-assembling rate

Man-Chien Chao · Chia-Hsien Chang · Hong-Ping Lin · Chih-Yuan Tang · Ching-Yen Lin

Received: 27 November 2008 / Accepted: 16 May 2009 / Published online: 11 June 2009

Abstract Pluronic 123-templated mesoporous SBA-15 silica rods with a length of ca. 3.0–4.0 μm were easily synthesized in a dilute silicate solution with a pH value of 2.0 at room temperature. Through a good control on the synthetic condition and the chemical components, a high homogeneity (>95%) of the hexagonal SBA-15 silica rods can be achieved. In addition, the effect of the synthetic conditions including acid source, weight ratio of the P123/sodium silicate, temperature, water content, pH value, and applying shearing flow were explored in detail to tailor the morphologies of the SBA-15 mesoporous silicas. In this paper, we also focused on the counterion effect on the synthesis of the SBA-15 mesoporous silicas. It was found that the SO_4^{2-} counterion from H_2SO_4 has higher affinity to induce the formation of P123 rod-like micelles than that of Cl^-, NO_3^-. Meanwhile, we postulated that the self-assembly pathway of the silica species and the neutral *tri*-block copolymer micelles in a dilute solution with a pH value of 2.0 would occur through an $S^0 \cdots I^0$ rather than the $S^0X^- \cdots I^+$ one as previously discussed. We further employed the SAB-15 mesoporous silica rods as the templates to synthesize high-quality CMK-3 mesoporous carbon rods by using commercially available phenol–formaldehyde (PF) resin as the carbon source.

M.-C. Chao
Department of Chemistry, National Taiwan University, Taipei 106, Taiwan

C.-H. Chang · H.-P. Lin (✉)
Department of Chemistry and Center for Micro/Nano Science and Technology, National Cheng Kung University, Tainan 701, Taiwan
e-mail: hplin@mail.ncku.edu.tw

C.-Y. Tang · C.-Y. Lin
Instrumentation Center, National Taiwan University, Taipei 106, Taiwan

Introduction

Since the discovery of mesoporous silicas by Yanagisawa et al. and the researchers in Mobil Oil Corporation, significant extensive progress has been made in the synthesis, characterization, and application of the mesoporous materials [1]. Typically, the mesoporous silicas were prepared by using either ionic or neutral surfactants as mesostructural templates. Recently, block-copolymer surfactants such as alkyl polyethylene oxide and Pluronic *tri*-block copolymers have been widely used to synthesize the mesoporous materials because of the advantages (e.g., biocompatibility, commercial availability, low cost, and nontoxicity) in comparison to ionic surfactants [2, 3]. For practical applications, fabrication of mesoporous silicas in a desired morphology is important as well as the controls in composition, pore structure, and porosity. Mesostructured materials in the form of films [4, 5], monolith [6, 7], sphere [8, 9], fiber [8, 10], crystals [11, 12], and platelets [13] have been obtained by using commercial nonionic block copolymers as supramolecular templates and organic silica source (e.g., TEOS).

Zhao and his co-workers [11, 14] have studied the SBA-15 rods in the high concentration of KCl salt, and a colloidal phase separation mechanism (CPSM) for the formation of mesoporous materials is proposed [15]. Until now, studies on the formation mechanism for mesostructured single crystals templated either by ionic surfactants [16–19] or by nonionic block copolymers [11, 12] have few been reported. Kosuge et al. [20] have synthesized rod-like and fiber-like

SBA-15 with well-defined morphologies and high mesoscopic ordering using a commercial sodium silicate solution and P123 *tri*-block copolymer in a highly acidic condition (pH < 1.0).

Recently, we have reported that alkyltrimethylammonium (C_nTMAB n = 14–18)-templated SBA-1 crystals in different shapes were readily synthesized in an acidified silicate solution at different pH values around 2.0 [21–23]. The relative areas of the (100) and (110) planes of the 3D cubic *Pm3n* mesostructure of SBA-1 is dependent on the pH value of the solution [21] or on the chain length of the surfactant C_nTMAX [22]. In this paper, we attempted to employ such moderate reaction condition (e.g., pH value = 2.0, room temperature) to synthesize the P123-templated SBA-15 silica in different morphologies by using highly dilute silicate solution as the silica source instead of using the organic silica source TEOS. Because the silica condensation rate is slowest at pH value around 2.0 which is close to the *iso*-electric point of silica, the P123 micelles and silica species can be allowed to self-assemble gradually to a thermodynamically stable SBA-15 hexagonal rod rather than the irregular particles [24].

Furthermore, the effect of counterion on the morphology of the P123-templated mesostructured silicas was explored as well. It is known that the micellar structure of the surfactant is dependent on the added salts. Distinct from the cationic surfactant, the concentration of the cloudy point of the nonionic surfactant decreases with the salting-out capability of the added salts. Consequently, adding different salts could offer a wide range of possibilities to tailor the morphology and surface properties of mesoporous silica. As the Hofmeister series, the length of the resulted SBA-15 mesoporous silica increases as the series $SO_4^{2-} > Cl^- > NO_3^-$ [25]. Based on the EDX data of the samples from different acidic sources, we also found that the assembly of the mesoporous silicas organized by nonionic *tri*-block copolymer species in such acid media occurs through an $(S^0)(H^+I^-)$ or (S^0I^0) pathway. Other effects of synthetic conditions which affect particle morphology, such as temperature, stirring rate, reactant ratios, and pH value upon the macrostructures of mesoporous silicas were discussed as well.

Experimental section

Materials

The silica source is sodium silicate (27 wt% SiO_2, 14 wt% NaOH, Aldrich) or tetraethyl orthosilicate (TEOS, Acrôs). The templating agent is nonionic *tri*-block copolymer, Pluronic 123 ($EO_{20}PO_{70}EO_{20}$), purchased from Aldrich. The sulfuric acid (H_2SO_4), nitric acid (HNO_3), and hydrochloric acid (HCl) are from Acrôs. Phenol–formaldehyde (PF) resole-resin PF650 (MW ca. 95,580, Chang-Chung Plastics, Taiwan) is used as the carbon source. All commercial chemicals were used directly without further purification.

Synthesis

In a typical synthesis of rod-like SBA-15 mesoporous silica, 2.0 g of Pluronic 123 (P123, $EO_{20}PO_{70}EO_{20}$) was dissolved in 50–200 g of H_2O at 30 °C to form a homogeneous solution. Then, the surfactant solution was poured into a dilute acidified silica solution with the pH value range of 1.0–3.0. The acidified silica solution was prepared by rapidly pouring a mixture of 8.26 g of sodium silicate and 50.0 g H_2O into 150 g of 0.5 M H_2SO_4 aqueous solution, and the pH value of the acidified solution was carefully adjusted to 1.0–3.0 by titrating a proper amount of 0.1 M NaOH solution. After stirring for 10 min, the surfactant–silica solution was subsequently kept under a static condition at 30 °C for 2–4 days. To prepare the fiber-like SBA-15 mesoporous silica, the reaction solution was continuously stirred. In addition, we investigated the counterion effect of the acid source on the morphology of mesoporous silicas. The synthetic process and the chemical composition were the same except varying acid sources, such as H_2SO_4, HNO_3, and HC1. To have the same equivalence of 0.5 M H_2SO_4, the concentration of HCl and HNO_3 is 1.0 M. The molar composition of the reaction mixture was: 1.0 $E0_{20}P0_{70}EO_{20}$: (2.15–8.60) SiO_2: 1.67 NaOH: (4.35–8.90) HX: (482–5790) H_2O.

When using the organic silica source of TEOS, the mole of the silica content in the added TEOS (the weight ≈ 7.7 g) is the same with that of sodium silicate. However, a pre-hydrolysis process is needed until TEOS/water phase separation disappeared and a homogeneous solution was obtained. After 6 days of aging at 30 °C, the solid products were filtrated and washed repeatedly with water. After drying at 60 °C for 1 day, the organic-template was removed by a 560 °C-calcination in air.

For getting a stable mesostructured carbon replica, the as-synthesized mesoporous silica rods were hydrothermally treated at 100 °C for 1 day to achieve an interconnected 3-D mesostructure [26]. The synthetic process of the mesoporous carbon replica is as follows: 2.0 g of phenol–formaldehyde (PF) resole-resin PF2180 (Mw ca. 95,580, Chang-Chung Plastics, Taiwan) was added into 30.0 g of ethanol to form a homogeneous solution. This PF ethanol solution was combined with 1.0 g of the calcined SBA-15 mesoporous silica rods hydrothermally treated at 100 °C for 1 day as a solid template for the mesoporous carbon, and continuously stirred for an appropriate time of (12–48) h. The mixture was dried at 100 °C for 12 h, and then a black gel-like product was formed after ethanol evaporation.

The resulted solid product was ground into powder-form and transferred into a quartz boat. The thermal-setting PF-resin containing mesoporous silica was carbonized in an oven under nitrogen atmosphere at a heating rate of 10 °C/min from the room temperature to 900 °C and maintained at 900 °C for (1.0–3.0) h. The silica framework was removed by HF (5.0 wt%) etching. After filtrating, washing, and drying the mesoporous carbons were obtained.

Characterization

Powder X-ray diffraction (XRD) patterns were obtained on Wiggler-A beam line ($\lambda = 0.1326$ nm) of the National Synchrotron Radiation Research Center at Hsinchu, Taiwan. The N_2 adsorption–desorption isotherms were obtained at 77 K on a Micromeritics ASAP 2010 apparatus. Before the analysis, the sample was outgassed at 200 °C for about 6 h in 10^{-3} torr. BET analysis was used to determine the total specific surface area (S_{BET}). The total pore volume (V_{total}) and micropore volume (V_{micro}) of the products were calculated by using a *t*-plot analysis. The mesopore diameter was calculated from the desorption branch of nitrogen isotherms by using the Broekhoff and de Boer (BdB) method [25]. The scanning electron microscopy (SEM) and transmission electron micrographs (TEM) were taken on an S-800 (Hitachi) operated at an accelerating voltage of 20 keV and an H-7100 (Hitachi) operated at an accelerating voltage of 100 keV, respectively. The organic surfactant content of the mesoporous silicas was measured by thermogravimetric analysis (TGA). TGA were conducted with a ULVAC TGA-7000RH thermogravimetric system. In a typical experiment, ca. 10 mg of sample was heated from the room temperature to 700 °C at 10 °C/min in air. The surfactant content was determined from the weight loss between the temperature ranges of 140–300 °C.

Results and discussion

General features of the synthesized P123-templated mesoporous silica

In the typical synthesis of P123-templated mesoporous silicas, the P123/H_2O/H_2SO_4/sodium silicate system was under a static condition for 2–4 days at pH value of 1.0–3.0. One can clearly see that the particles morphologies were highly sensitive to reaction pH (Fig. 1a–c), even in a narrow pH region from 1.0 to 3.0. At pH = 2.0 close to the *iso*-electric point of silica (pH ≈ 2.0), the silica condensation is the slowest [24]. Thus, a long reaction time allows

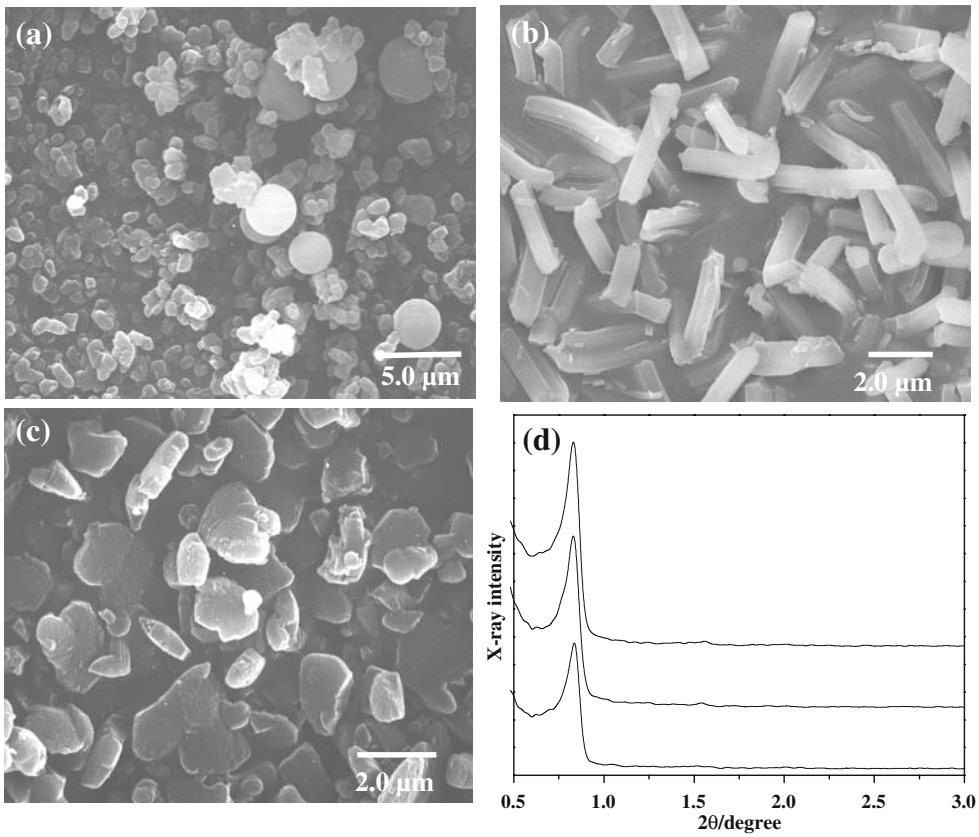

Fig. 1 SEM images and XRD patterns of the mesoporous silicas synthesized with the P123/silica/H_2SO_4/H_2O silicate composites at different pH values. **a** 3.0, **b** 2.0, **c** 1.0. **d** XRD patterns of the samples in (**a**, **b**, and **c**)

the P123 micelles and silica species to assemble into the thermodynamically stable rod-like morphology. Out of this pH value, the silica condensation is relatively fast, and then the irregular particles were generated instead. Although these samples are in different morphologies, all of these samples possess the representative XRD patterns of 2-D hexagonal mesostructure (Fig. 1d). According to these results, the equilibrium rod-like morphologies in micrometer-scale required longer assembling time than that for the mesostructural arrangement in nanometer-scale.

Figure 2a reveals the XRD profile of rod-like morphology of P123-templated mesoporous silica shows similar patterns of the 2-D hexagonal symmetry (*p6mm*) with conventional SBA-15 materials. Figure 2b and c displays the microtome transmission electron microscopy (TEM) images of the rod-like silica sample of Fig. 1b. Figure 2b shows that the rod-like particles are ca. 500 nm in diameter. The silica rod consists of numerous nanochannels running parallel to the long axis (along the [110] axis) and does not have obviously topological defects. The clear cross-section images show that nanochannels are perfectly stacked to form an equilibrium hexagonal morphology (Fig. 2b and c). The parallel stripes in these images demonstrated regular stacking of elongated micelle assemblies of the synthesized rod-like silicas by using H_2SO_4 as acid source. From analyzing the thermogravimetric analysis profile of the as-synthesized rod-like samples, we found the weight loss between 120 and 400 °C is about 40–55 wt%. The P123/silica ratio is close to the typical SBA-15 materials reported in the previous literatures. The organic template/silica weight ratio in the as-synthesized mesocomposite is close to 1.0 that indicates the P123 surfactant and the silica species homogeneously assemble without forming the surfactant-free amorphous silica particulates. The nitrogen adsorption/desorption isotherm (Fig. 2d) of corresponding material is ascribed to a type IV isotherm with a type-H1 hysteresis loop, which is characteristic of a typical mesoporous material with 1-D cylindrical channels. The calcined rod-like SBA-15 has a pore size of 5.3 nm (calculated from the adsorption branch by the BJH model), a BET surface area of 438 $m^2\ g^{-1}$, and a pore volume of 0.45 $cm^3\ g^{-1}$.

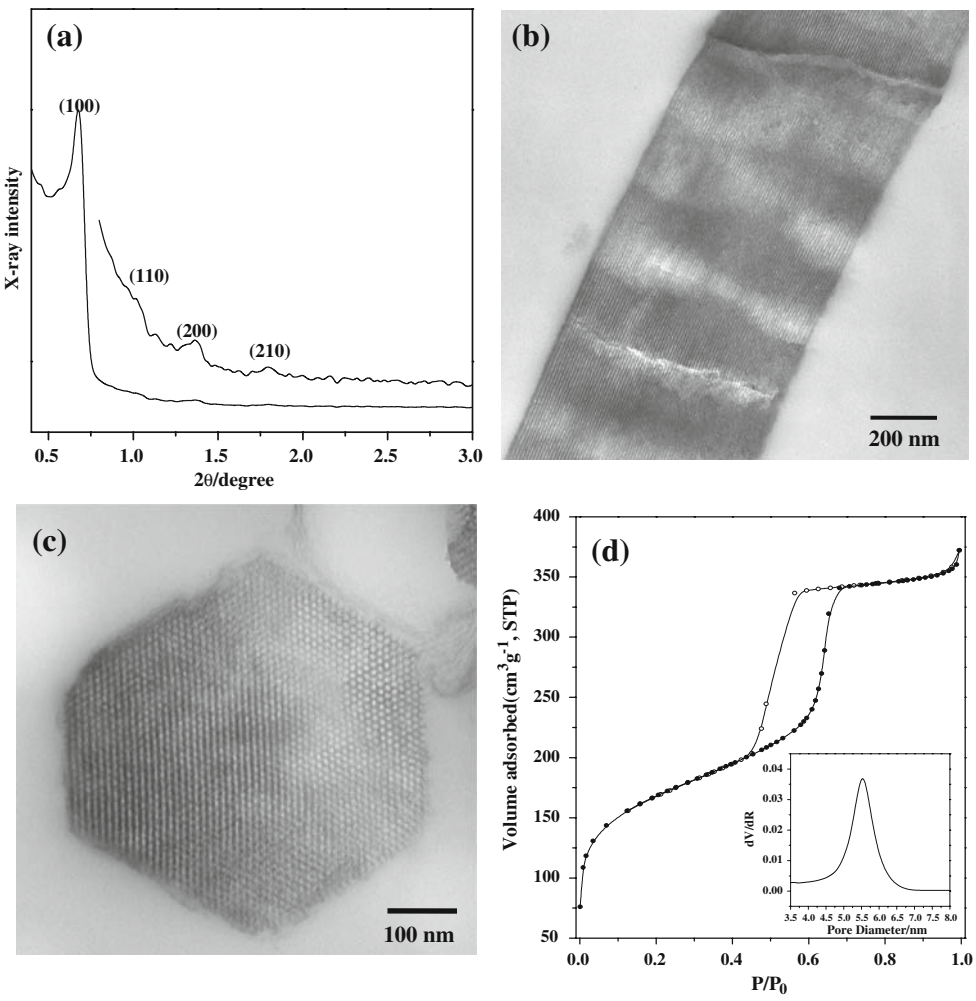

Fig. 2 **a** XRD profile of the calcined rod-like SBA-15 sample while the weight ratio of $P123/SiO_2 = 1.0$ at 30 °C under static condition; **b** microtome TEM micrographs of rod-like SBA-15 sample, **c** a cross-sectional image along (100) direction, **d** nitrogen adsorption/desorption isotherm, the inset diagram is pore size distribution curve

From SEM and TEM observations (Figs. 1 and 2), we can prepare the rod-like morphology of P123-templated mesoporous silicas in a high homogeneity ~100% under quiescent conditions at the appropriate pH value of 2.0. Another important factor for the synthesis of rod-like SBA-15 is to use a large amount of water in comparison to that used in the ingredients of the particle-like SBA-15. The dilute synthetic condition would also slow down the self-assembling rate of surfactant and silica species to provide a time long enough for the equilibrium-assembly of micro-sized rod-like silicas. Thus, the induction periods are rather long, often in days. After 2–4 days, the silica recovery is high and close to 80 wt% of the added silica source. As in our previous report [12], we have synthesized the faceted

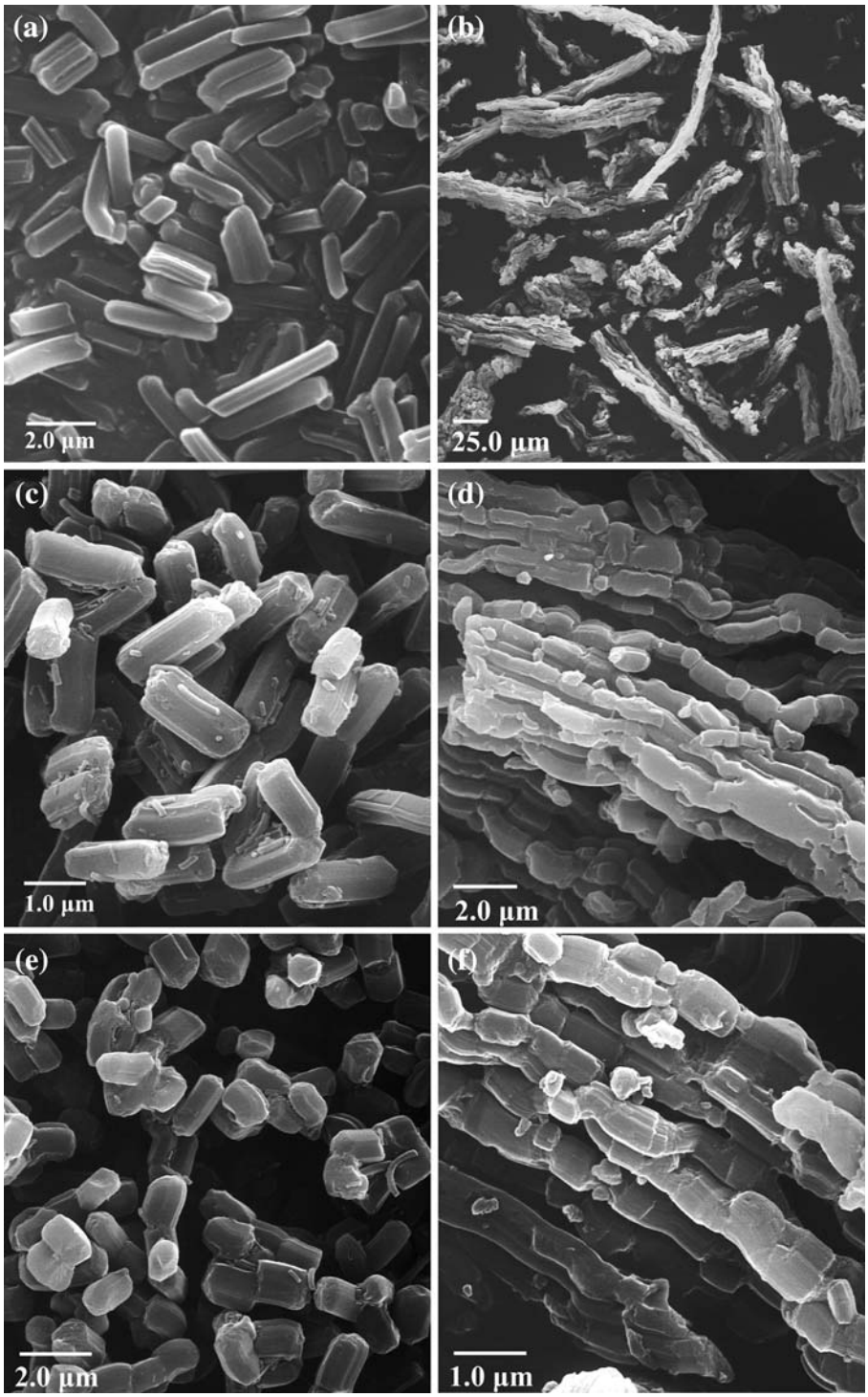

Fig. 3 SEM images of the rod-like and fiber-like silica products by using different acid sources under stirring or static conditions. **a** H_2SO_4, static; **b** H_2SO_4, under stirring; **c** HCl, static; **d** HCl, under stirring; **e** HNO_3, static; **f** HNO_3, under stirring

single crystals of rhombdodecahedron form of SBA-16 morphology by using the surfactant system C_8TMAB/SDS/F127 as template in a dilute solution. Pang and his coworkers [27, 28] have reported hexagonally faceted MCM-41 morphology using extremely dilute surfactant concentration. Cai et al. [27, 28] have studied MCM-41 rods in dilute basic medium.

In sum, there are two synthetic procedures involved in the organization of the mesostructure: the surfactant/silicate self-assembly and the silica condensation. One may need a well-separated time scale of the above two processes in order to have high-quality morphology control. If the silica condensation rate were too fast, one would be trapped in non-equilibrium structure (irregular form) before the structural relaxation of the liquid crystalline phase is complete. To have a good equilibrium structure, one has to slow down the silica condensation. A good control on the pH value and dilution provide a convenient approach to synthesize the rod-like SBA-15 mesoporous silica. Many synthetic factors having strong influence upon the morphologies of the P123-templated mesoporous silicas, such as acid source, shearing flow, and pH control (acidity), will be further discussed in the following paragraphs.

Counterion effect of the inorganic acid source

Previously, Pinnavaia and his coworkers [29–31] used nonionic surfactants to synthesized disordered, worm-like mesoporous silica under neutral pH conditions, and proposed an S^0I^0 mechanism involving hydrogen-bonding interactions between the surfactant and siloxane species. Zhao et al. [2] have studied the effects of the radius and charge of the anion (X^-) and the strength of acid on the assembling rate of the *tri*-block copolymer and silica. Therefore, they postulated that the assembly of the mesostructure of silica species and nonionic *tri*-block copolymer in acid media occurs through an $(S^0H^+)(X^-I^+)$ pathway. Recently a few literatures have discussed the effect of counterion (X^-) on the morphological control in the acidic synthetic condition by using nonionic *tri*-block copolymers as template. In this paragraph, we explored the influence of the counterion of the acid source on the morphology of the P123-templated mesoporous silica. Three different acid sources including H_2SO_4, HNO_3, and HC1 were used and pH value of the solution was set at 2.0.

SEM images of the SBA-15 samples prepared with different acid sources are displayed in Fig. 3a, c, and e. The morphologies of all the products obtained from different acid sources are in a rod-like form, only different in length. While using H_2SO_4 as the acid source, we can obtain rod-like mesoporous silicas with a relatively uniform size of ca. 2–4 μm in length, which is longer than those prepared with HCl and HNO_3 as the acid source. This result is different from that reported by Kosuge et. al. [20]. Our results suggested that the more polarizable SO_4^{2-} counterion has stronger binding strength onto polyoxyethylene chain of the P123 surfactant than that of Cl^- or NO_3^- ion. The existence of the SO_4^{2-} would induce the formation of more elongated micelles. Then, the longer micelles can be perfectly stacked to form a hexagonal rod-like morphology with longer length. Therefore, we found that the counterion effect of the acid sources on the length of the SBA-15 mesoporous silicas get the series $SO_4^{2-} > Cl^- > NO_3^-$. This tendency is relative to the salting out affinity toward the micellization of the P123 surfactants and the decrease of the cloudy point of the nonionic P123 *tri*-block copolymer surfactant [25]. Form the examination on the XRD patterns, we found all these samples possess the 2-D hexagonal *p6mm* mesostructure. The physical properties of these materials are

Table 1 Physical properties of the rod-like and fiber-like mesoporous silicas prepared with P123/H_2O/acid/sodium silica compositions by using different acid sources at 30 °C under pH value around 2.0

Samples	EDX X/Si (X = S, Cl, N)	a_0 (nm)	S_{BET} (m^2 g^{-1})	D_{BdB}[b] (nm)	t[c] (nm)	V_{micro} (cm^3 g^{-1})	V_{meso} (cm^3 g^{-1})
Static condition							
H_2SO_4-made	0	10.5	438	7.3	3.6	0.076	0.446
HCl-made	0	10.6	515	7.8	3.2	0.093	0.541
HNO_3-made	0[a]	10.6	407	7.6	3.4	0.054	0.448
Stir condition							
H_2SO_4-made	0	10.5	566	7.6	3.3	0.135	0.544
HCl-made	0	10.5	505	7.6	3.3	0.108	0.498
HNO_3-made	0[a]	10.5	517	7.7	3.2	0.107	0.535

[a] The nitrogen/silicon ratio was measured using an element analyzer

[b] Mesopore diameter (D_{BdB}) = 1.05 a_0 $\varepsilon_{meso}^{1/2}$; $\varepsilon_{meso} = V_{mes}/(V_p + 1/\rho_{Si})$; $V_p = V_{mes} + V_{micro}$; ρ_{Si} = 2.2 cm^3 g^{-1}

[c] Wall thickness (t) = a_0 − 0.95 D_{BdB}

listed in Table 1. Basically, all of these rod-like samples exhibit large surface area (435–520 m^2 g^{-1}) and uniform pore size (5.0–5.5 nm), which are similar to the usual SBA-15 silica. We also notice that the rod-like mesoporous silica materials contain a fraction of micropore volume which is about 12–17% of the total pore volume whatever be the acid source used (see Table 1).

In some recent literatures [2], the model of (S^0H^+) (X^+I^-) pathway has been widely adopted to explain the formation of the nonionic surfactant–silica composites. To check whether this concept could also be applied to our synthetic system, we analyzed the amount of the counterion in the as-synthesized samples prepared with different acid sources by using energy dispersive X-ray analysis (EDX). The EDX data were also showed in Table 1. However, the residual amounts of the S and Cl elements forming SO_4^{2-} and Cl^- counterions in the solid-form products are too low to be detected. In parallel, from the analysis of the element analyzer (EA), we found that no N element exist in the solid product of the P123-templated mesoporous silica synthesized with HNO_3 as acid source. When using HBr as acid source, no Br^- ion in the product can be detected by titrating the gel solution of the as-synthesized product with $AgNO_3$ solution (no AgBr precipitate) and EDX analyzing. Based on these results, we reasonably postulated that the assembly of the mesoporous silicas organized by nonionic *tri*-block copolymer micelles should occur though an $(S^0\cdots I^0)$ pathway under the synthetic condition we provided. Therefore, we can conclude that the counterion would exist in the intermediate at the early stage rather than in the resulted SBA-15 silica products.

Effect of shearing flow

Slow assembling rate is needed for the formation of rod-like silicas under the static condition. It is known that applying shearing flow can promote the alignment of the rod-like micelles. Figure 3b, d, and f are SEM images of the mesoporous silica products under stirring. It is clearly seen that most of the mesoporous silica products are in fibrous morphology with fiber lengths ranging from tens to few hundreds micrometers even by using different acid sources (e.g., H_2SO_4, HNO_3, and HC1). These fiber-like products comprise bundles of micro-sized rod shown in Fig. 3a, c, and e. According to these results, it is clear that the macroscopic morphologies of the fiber-like products are governed by the stirring effects during the formation of the P123 *tri*-block copolymer cylindrical micelles-templated silica. Stirring is the indispensable factor for elongating the fiber-like silicas, e.g., fibrous SBA-15 [8, 31–33] and MCM-41 [32]. In contrast, static conditions are essentially needed to obtain a high yield of well-faceted

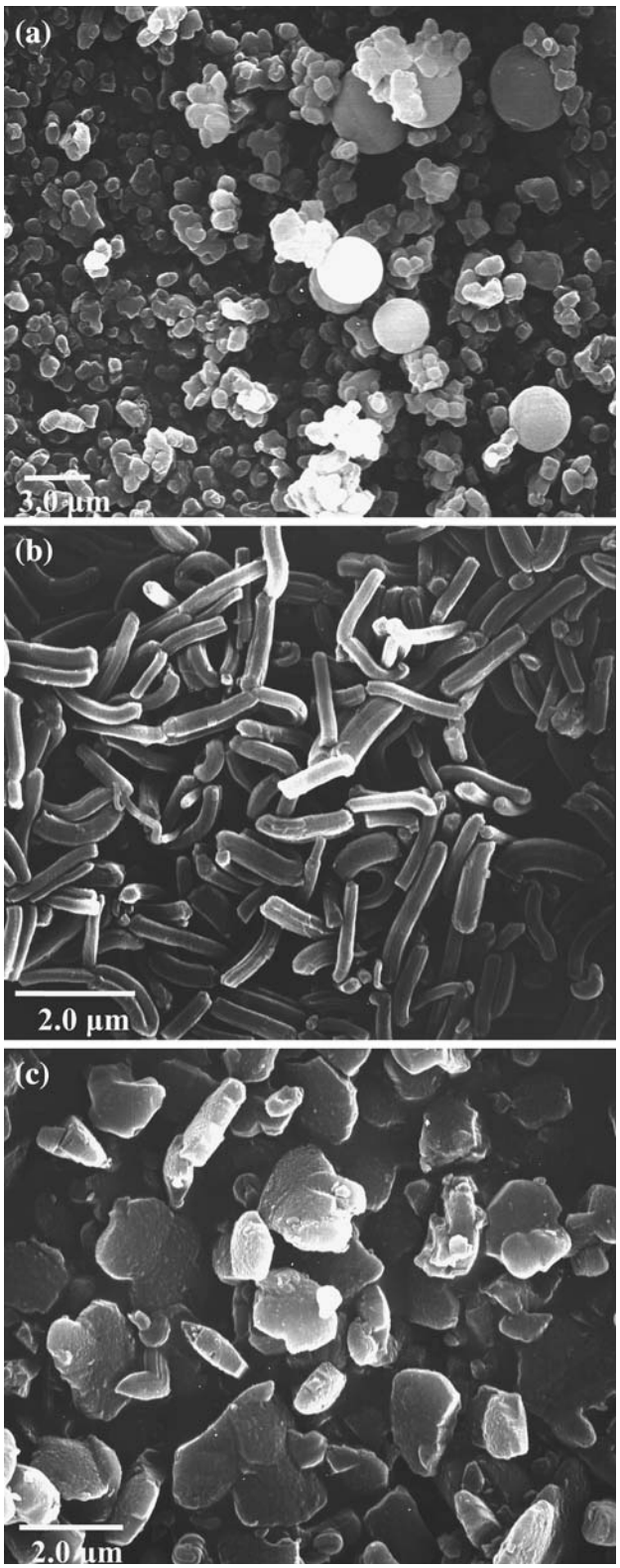

Fig. 4 SEM micrographs of the as-synthesized rod-like SBA-15 materials by using P123/H_2SO_4/H_2O/sodium silicate system in various weight ratios of P123/SiO_2 at 30 °C under pH value of 2.0 without stirring condition. **a** P123/SiO_2 = 0.5, **b** P123/SiO_2 = 1.0, **c** P123/SiO_2 = 2.0

crystals with 3-D mesostructures templated by the spherical micelles [22, 23]. If the solution were stirred, the well packing of the spherical building blocks would be destroyed. The crystal-like morphology would then thus be defect-dominated.

P123/SiO_2 ratio

Figure 4 demonstrates SEM images of the as-synthesized samples prepared at different P123/SiO_2 weight ratio by using H_2SO_4 as acid source and depend on the pH value of 2.0. When the ratio of P123/SiO_2 is about 1.0, we can conveniently obtain mesoporous silica rods with a relatively uniform size of ca. 0.5–0.7 μm in width and ca. 2–4 μm in length (Fig. 4b). These samples are composed of almost ~100% rod-like particles in morphology. On the contrary, the morphology of the silica products prepared at lower or higher P123/SiO_2 ratios are transformed to monoliths (Fig. 4a; at P123/SiO_2 = 0.5) or particles (Fig. 4c; at P123/SiO_2 = 2.0). Consequently, the P123/SiO_2 weight ratio is also an important factor for the formation of the rod-like mesoporous silicas.

Using the TEOS as the silica source

In addition to the acidified sodium silicate solution, the organic silica source of TEOS is usually performed to synthesize the rod-like SBA-15 silicas in acidic solution. Because the TEOS is hydrophobic, several-hour stirring is needed to allow the partial hydrolysis of the TEOS to form the water-soluble silica species. We found that the rod-like and particle morphology of the SBA-15 samples were also synthesized with the P123/H_2SO_4/H_2O/TEOS compositions (Fig. 5a). The length of the TEOS-made mesoporous silica rods is in submicron size. In a more dilute condition, one can get silica nanorods about 300–600 nm in length and ca. 100 nm in diameter (Fig. 5b), and the result is similar to that have been reported [8].

$$\mathrm{Si(OEt)_4} \xrightarrow{\text{Hydrolysis}} \mathrm{Si(OEt)_{4-x}(OH)_x} \xrightarrow{\text{Condensation}} \text{Silica Species} \quad (1)$$

Different from using the sodium silica, a longer reaction time is essentially required to obtain the TEOS-made SBA-15 mesoporous silica. This is because an additional hydrolysis process is essentially needed from TEOS to silica species (Eq. 1). Due to the low concentration of the TEOS and surfactant, the hydrolysis rate is relatively slow, and then a long reaction time (≈6 days) is necessary.

SBA-15 silica rods as nanotemplate of CMK-3 mesoporous carbon

These silica rods have been utilized as templates to make mesoporous carbon materials. The commercially available phenol–formaldehyde (PF) resin was used as the carbon source [34–36]. Figure 6a shows the representative transmission electron microscopic (TEM) images of the mesoporous carbon. One can clearly see the well-ordered mesostructure of the rod-like CMK-3 samples as same as that of the solid template of the SBA-15 rods (Fig. 2b). The carbon nanorods run parallel to the fiber axis. Three well-resolved XRD peaks are observed in the resulted mesoporous carbon, which can be assigned to (100), (110), and (200) reflections of the 2D hexagonal mesostructure (*p6mm*) (curve II of Fig. 6b). The well-ordered mesostructure in the rod-like mesoporous carbon confirms that the thermal setting PF resin is an alternative carbon source to replicate the mesoporous silica. The nitrogen adsorption/desorption isotherm of the CMK-3 rod-like carbon are type IV with type H1 hysteresis loop (not shown). The carbon has a pore size of 4.5 nm, a BET surface area of

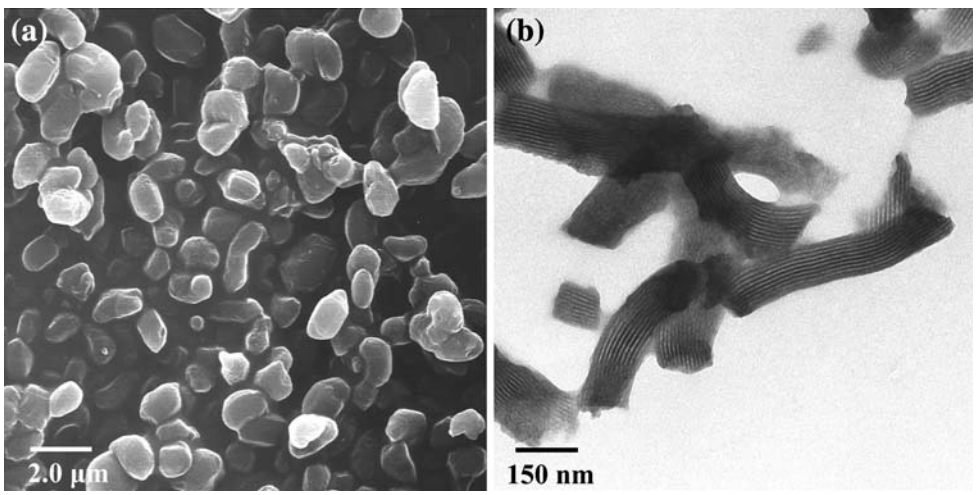

Fig. 5 SEM images of the mesoporous silica using P123/H_2SO_4/H_2O/TEOS system of different water content at weight ratio P123/SiO_2 = 1.0. **a** H_2O = 200 mL, **b** H_2O = 400 mL

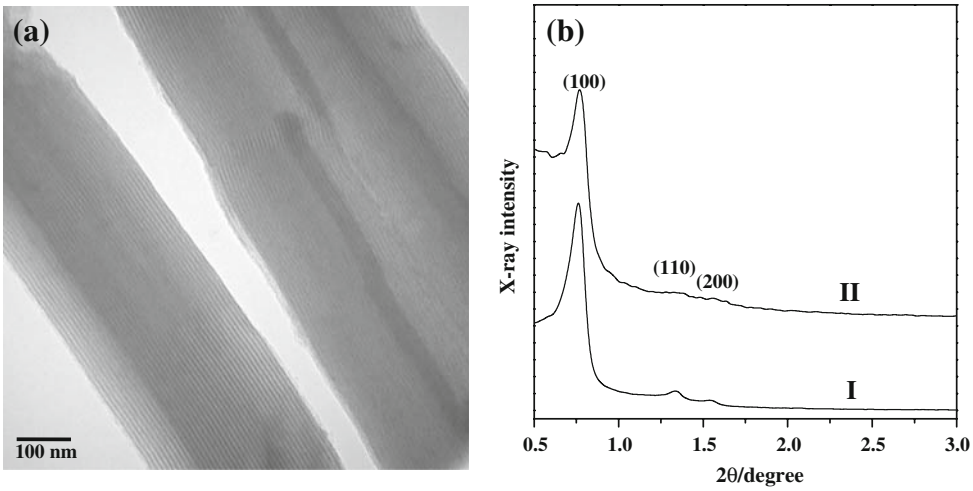

Fig. 6 **a** TEM image of as-synthesized rod-like CMK-3 mesoporous carbon synthesized by using rod-like SBA-15 after a hydrothermal treatment at 100 °C as templates, **b** XRD profiles: I. calcined SBA-15 rods after a hydrothermal treatment at 100 °C for 1 day, II. CMK-3 mesoporous carbon synthesized with sample I

981 $m^2\ g^{-1}$, and a pore volume of 0.99 $cm^3\ g^{-1}$. Lin and his coworkers [32] have reported the high-quality mesoporous carbons with different pore size, mesostructures, and morphology using cheap, commercially available PF resin as an alternative carbon source. This method also opens a novel route for mass production of mesoporous carbons in potential applications.

Conclusion

In brief, we have proposed a convenient method to synthesize P123-templated SBA-15 silica fibers in a highly diluted sodium silicate solution at pH = 2.0. The length of the fibers can be changed by applying a shearing flow and using different acid sources. In addition, a new S^0I^0 formation model was proposed to explain the formation of SBA-15 mesoporous silicas. The main factors for controlling the morphologies of SBA-15 silicas have been discussed as well. With a good control of assembling kinetics, one can judiciously manufacture the mesoporous silicas. Moreover, the mesoporous SBA-15 silica fibers with an interconnected mesostructure can be used as a hard template to synthesize the mesoporous carbon fibers with high surface area and porosity via a simple impregnation of phenol–formaldehyde polymer and silica removal. These mesoporous silicas and carbons have potential applications in catalyst, absorbent, sensor, magnetically separable carrier, micro-capsules, super-capacitor, drug delivery, electrode materials in fuel cells, and hard template for mesoporous metal oxides.

Acknowledgements Authors thank Chung-Chun Plastic, Taiwan, for providing PF polymers. This research is financially supported by National Science Council of Taiwan (NSC95-2113-M-006-011-MY3 and NSC95-2323-B-006-008) and Taiwan Textile Research Institute and Landmark Project from National Cheng Kung University (R017).

References

1. Kresge CT, Leonowicz ME, Roth WJ, Vartuli JC, Beck JS (1992) Nature 359:710
2. Zhao D, Feng JL, Huo QS, Melosh N, Fredrickson HG, Chmelka BF, Stucky GD (1998) Science 279:548
3. Zhao D, Huo QS, Feng JL, Chmelka BF, Stucky GD (1998) J Am Chem Soc 120:6024
4. Zhao D, Yang P, Melosh N, Feng J, Chmelka BF, Stucky GD (1998) Adv Mater 10:1380
5. Miyata H, Noma T, Watanabe M, Kuroda K (2002) Chem Mater 14:766
6. Feng PY, Bu XH, Stucky GD, Pine DJ (2000) J Am Chem Soc 122:994
7. Yang HF, Shi QH, Tian BZ, Xie SH, Zhang FQ, Yan Y, Tu B, Zhao D (2003) Chem Mater 15:536
8. Zhao D, Sun JY, Li QZ, Stucky GD (2000) Chem Mater 12:275
9. Boissiere C, Larbot A, van der Lee A, Kooyman PJ, Prouzet E (2000) Chem Mater 12:2902
10. Yang PD, Zhao DY, Chmelka BF, Stucky GD (1998) Chem Mater 10:2033
11. Yu CZ, Tian BZ, Fan J, Stucky GD, Zhao DY (2002) J Am Chem Soc 124:4556
12. Chen BC, Chao MC, Lin HP, Mou CY (2005) Microporous Mesoporous Mater 81:241
13. Chen BC, Lin HP, Chao MC, Mou CY, Tang CY (2004) Adv Mater 16:1657
14. Yu C, Fan J, Tian B, Zhao D, Stucky GD (2002) Adv Mater 14:1742
15. Yu C, Fan J, Tian B, Zhao D (2004) Chem Mater 16:889
16. Kim JM, Kim SK, Ryoo R (1998) Chem Commun 259
17. Guan S, Inagaki S, Ohsuna T, Terasaki O (2000) J Am Chem Soc 122:5660
18. Che S, Sakamoto Y, Terasaki O, Tatsumi T (2001) Chem Mater 13:2237
19. Trikalitis PN, Rangan KK, Bakas T, Kanatzidis MG (2002) J Am Chem Soc 124:12255
20. Kosuge K, Sato T, Kikukawa N, Takemori M (2004) Chem Mater 16:899
21. Chao MC, Wang DS, Lin HP, Mou CY (2003) J Mater Chem 13:2853
22. Chao MC, Lin HP, Wang DS, Mou CY (2004) Chem Left 33:672
23. Chao MC, Wang DS, Lin HP (2005) Microporous Mesoporous Mater 83:269
24. Lin HP, Mou CY (2000) Acc Chem Res 35:927

25. Leonidis E (2002) Opin Curr Coll Int Sci 7:81
26. Galarneau A, Cambon H, Renzo FD, Ryoo R, Choi M, Fajula F (2003) New J Chem 27:73
27. Cai Q, Lin WY, Xiao FS, Pang WQ, Chen X, Zou BS (1999) Microporous Mesoporous Mater 32:1
28. Cai Q, Luo ZS, Pang WQ, Fan YW, Chen XH, Cui FZ (2001) Chem Mater 13:258
29. Bagshaw SA, Prouzet E, Pinnavaia TJ (1995) Science 269:1242
30. Bagshaw SA, Pinnavaia TJ (1996) Angew Chem Int Ed Engl 35:1102
31. Prouzet E, Pinnavaia TJ (1997) Angew Chem Int Ed Engl 36:516
32. Schmidt-Winkel P, Yang P, Margolese DI, Chmelka BF, Stucky GD (1999) Adv Mater 11:303
33. Chao MC, Lin HP, Sheu HS, Mou CY (2002) Stud Surf Sci Catal 141:87
34. Lin HP, Liu SB, Mou CY, Tang CY (1999) Chem Commun 253
35. Lin HP, Kao CP, Liu SB, Mou CY (2000) J Phys Chem B 104:7885
36. Lin YP, Lin HP, Chen DW, Liu HY, Teng H, Tang CY (2005) Mater Chem Phys 90:339